Paper No.
02004

CORROSION 2002

EVALUATION OF CORROSION INHIBITORS IN COOLING WATER SYSTEMS USING A COUPLED MULTIELECTRODE ARRAY SENSOR

Lietai Yang and Darrell Dunn
Center for Nuclear Waste Regulatory Analyses
Southwest Research Institute
San Antonio, TX 78238

ABSTRACT

A multielectrode localized corrosion sensor has been developed for evaluating the performance of corrosion inhibitors for carbon steel in cooling water. Experimental results indicate that the coupled multielectrode sensor provided instantaneous measurement of corrosion currents and a rapid real-time response to the addition of inhibitors. Evaluation of several inhibitors showed that the sensor was able to distinguish between inhibitor type and concentration. It was also demonstrated that the sensor has a detection limit of $5x10^{-11}$A with respect to current measurement. The capabilities of the sensor may be suitable for online monitoring of corrosion in a variety of applications where real-time monitoring is required.

Keywords: Coupled multielectrode sensor; galvanically coupled sensor; multiple electrode array sensor; localized corrosion sensor; localized corrosion probe; localized corrosion monitoring; wire beam electrode.

INTRODUCTION

The majority of corrosion phenomena encountered in practical applications are non-uniform or localized[1]. However, many of the effective on-line monitoring techniques such as the electrical resistance method[2-4] and linear polarization method[5, 6]are good for uniform, but not adequately sensitive to localized corrosion. Electrochemical noise method has been used for the measurement of pitting[7] and crevice corrosion[8]. Although it is a useful method to indicate the electrochemical activity of localized corrosion, there is no consistent dependence between the measured signals, such as the pitting index, and the localized corrosion rate[9,10]. The differential flow cell method[11-14] employing essentially two or more

electrodes that are made of identical corrodible metals relies on the measurement of the current through a zero resistance ammeter which couples the electrodes together, to predict localized corrosion. As this method requires the forced movement of the electrode or the solution, especially the cathode relative to the solution, the current between the slow moving anode and the fast moving cathode does not represent the true corrosion current flowing from a corroding site to a non-corroding site of a metal under localized corrosion. Furthermore, localized corrosion, pitting for example, usually focuses on an area that is significantly smaller than the large slow moving electrode (0.3 to 0.5 cm^2) used in the differential flow cell. Prediction of the localized corrosion damage based on the current measured from a large surface area may not be reliable. This paper presents the real-time measurement results obtained during the evaluation of corrosion inhibitors for carbon steel corrosion in cooling water using a coupled multielectrode sensor[15].

EXPERIMENTS

The schematic diagram of the coupled multielectrode array sensor is given in Figure 1. It is similar to the coupled wire beam electrode used by previous investigators[16,17] except the coupling of the electrodes are through resistors, which allow the use of a high resolution voltmeter instead of a zero resistance ammeter. The principle of this sensor and the auto-switching and electrode location mapping software have been described previously[18]. All sensing electrodes were made from 1-mm diameter 1010 carbon steel (UNS G10100) wire. The insulation on the wire sensing elements was either epoxy, or PTFE film. The sensors were polished to 600 grit prior to the start of every test. Two commercial corrosion inhibitors for carbon steel in cooling water systems, called Type A, and B in this paper respectively, and several chemical compounds that are known to have corrosion inhibiting effect were used in the experiments. The Type A inhibitor is a molybdate based and the Type B inhibitor is a nitrite based. The chemical compounds are sodium nitrate[19] and benzotriazole (BZA)[20].

The experiments were conducted in a 3-L glass cell, filled with 2 L tap water, at room temperature. Typical chemical analysis results of the tap water are given in Table 1. The tap water was aerated, by bubbling compressed CO_2-free air, for at least 1 hour before the start of the experiment. Continuous aeration was maintained during the course of the experiment. The solution was also manually stirred every time an inhibitor was added to the cell.

RESULTS

Commercial Inhibitors

Figures 2 and 3 show typical responses of the currents measured from the different electrodes of the coupled multielectrode sensors to the additions of commercial inhibitors. Figure 2 also shows the sensor currents when the sensor was placed in air and in de-ionized water. The signals for Figure 2 were obtained with 24-electrodes that were freshly polished prior to the start of the measurement. The signals shown in Figure 3 were obtained from an eight-electrode sensor. As shown in Figure 2 the currents from the 24-electrodes increased slightly when the sensor was changed from air to de-ionized water and increased significantly with the most negative current (maximum anodic current) reaching 3.0×10^{-6} A when the sensor was changed to tap water. Shortly after the sensor was immersed in tap water, a peak of maximum anodic current was recorded. Afterwards, the current decreased slightly and approached a steady state value of approximately 2.4×10^{-6} A. The decrease in current is consistent with the formation of corrosion products on the electrode surfaces. Immediately after the addition of the Type A commercial inhibitor, the most negative current decreased abruptly to 1×10^{-7} A. As shown in Figure 3, the most negative current of the eight-electrode sensor decreased sharply upon the addition of the Type

B commercial inhibitor to the tap water. The monitored response of the sensor electrodes revealed no increase in current many hours after the inhibitors were added and suggested continuous suppression of corrosion.

As reported earlier[18], the currents measured from a 25-electrode Type 304 (UNS S30400) stainless steel sensor can be described by normal distribution. Therefore, the standard deviation of the measured currents from the multielectrode sensor can be used to estimate the current that is the most anodic among the measured values. Thus the standard deviation is an effective indicator for localized corrosion. The standard deviation signals corresponding to Figures 2 and 3 and the more detailed inhibitor addition information are given in Figures 4 and 5. As shown in Figure 4, the standard deviation of the 24 currents shown in Figure 2 decreased from 6.5×10^{-7} to 2.0×10^{-8}A immediately after the addition of 2.5 ml/L inhibitor A and gradually decreased to about 1.8×10^{-8} A in about 18 hours. Further addition of the inhibitor up to 7.5 ml/L had no improvement on the inhibition effect. Figure 2 also shows that the sensor signal with the respect to the standard deviation in air is approximately 1×10^{-8} A. This high value might be due to the corrosion of the carbon steel electrodes under water film that was not properly removed after the exposure in the de-ionized water. A measurement in air at the end of the same experiment verified that the background sensor signal with the respect to the standard deviation was approximately 5×10^{-11} A when the sensor electrodes were carefully dried. This indicates that the sensor has a detection limit at least $5\text{x}10^{-11}$ with respect to corrosion current. As shown in Figure 3, significant inhibition effects started at the concentration of the Type B commercial inhibitor as low as 0.25 ml/L. After the addition of 0.25 ml/L, the standard deviation of the 8 currents as shown in Figure 3 decreased from 1×10^{-7} to 2×10^{-9}A. Further addition of the Type B commercial inhibitor at concentrations up to 8 ml/L had no improvement on the inhibition effect.

Further experiment with small step changes in the concentration of the Type A commercial inhibitor shows that the minimum effective concentration of the inhibitor in the test environment is between 0.5 to 1.5 ml/L. Although the sensor used to obtain the results as shown in Figure 6 is the same as that used for the results shown in Figure 4, the standard deviation of the currents in tap water as shown in Figure 6 are significantly lower than those as shown in Figure 4. This might be because the history of the sensor electrodes for Figure 6 is different from the history of the sensor electrodes for Figure 4. Prior to the experiment for Figure 6, the sensor had been used in the experiment for the evaluation of the Type A commercial inhibitor (Figures 2 and 4). Although the sensor electrodes were washed in water using soft brush and rinsed with de-ionized water for several times, traces of the Type A commercial inhibitor may still present on the surfaces of the electrodes after the Type A inhibitor exposure and the sensor electrodes had became less susceptible to localized corrosion than the freshly polished surface.

Other Inhibitors

The measured responses of the standard deviation signals of the carbon steel sensors to the addition of $NaNO_3$ and Benzotriazole (BZA) are shown in Figures 7 and 8 respectively.

The localized corrosion indicator of the sensor, standard deviation of currents, as shown in Figure 7 suggests that $NaNO_3$ is not effective for the inhibition of localized corrosion of 1010 carbon steel under the test conditions. The standard deviation of the current was approximately 6.0×10^{-7} A after exposure to fresh tap water. The addition of 50 ppm $NaNO_3$ resulted in a slight decrease in the standard deviation of the current. Increasing the $NaNO_3$ concentration to 1000 and subsequently 2000 ppm decreased the standard deviation of the current by a factor of 3. After the addition of up to 4000 ppm (wt) $NaNO_3$, the standard deviation was still above 1×10^{-7} A.

Figure 8 shows the localized corrosion indicator of the sensor obtained for the BZA inhibitor test. Without the addition of the inhibitor, the standard deviation of the current is near 5.0×10^{-7} A. Addition of either 50 or 100 ppm BZA did not result in a substantial decrease in current. The addition of 500 ppm BZA decreased the standard deviation of the current to less than 6×10^{-9} A. Subsequent increases in the concentration of BZA resulted in slightly lower currents with the lowest measured standard deviation of the current near 2×10^{-9} A. These results suggest that BZA is inhibitive at a concentration between 100 to 500 ppm(wt).

DISCUSSIONS

The preliminary results obtained in this study indicate that the galvanically coupled multielectrode sensor can be used to evaluate the effectiveness of inhibitors. The response of the sensor was dependent on both the type of inhibitor used and the concentration of the inhibitor. The results shown in Figure 4 indicate that 2.5 mL/L of inhibitor A is sufficient to provide an inhibiting effect for carbon steel. Increasing the inhibitor concentration did not result in a decreased standard deviation of the sensor currents. As shown in Figure 5, inhibitor B was more effective than inhibitor A. With 0.25 mL/L, the standard deviation of the carbon steel sensor currents was reduced to values that were 10 times less than observed with inhibitor A. Low standard deviation signal was also observed with BZA (Figure 8). On the other hand, the probe did not indicate that $NaNO_3$ was an inhibitor for carbon steel in tap water.

Because the composition of the commercial inhibitors used in this study are not known, a comparison of the inhibitor performance can only be made by comparing the value of the standard deviation of the current with and without the addition of inhibitor. It should be noted however that the concentration of the inhibitors used to suppress corrosion is not trivial. For many applications such as cooling water systems, the inhibitor concentration necessary to suppress corrosion may exceed allowable environmental restrictions. In these cases the careful selection of inhibitor and continuous monitoring of corrosion may be necessary to protect the component and maintain compliance with environmental restrictions. The response of the multielectrode sensor allows the evaluation of inhibitor performance, which may be useful in the selection of inhibitor. In addition, the sensor can potentially be used for on-line monitoring of corrosion rates to insure that sufficient inhibitor concentrations are used to prevent corrosion without the use of excess inhibitor concentrations.

The on-line monitoring of a corrodible component such as a heat exchanger or cooling water tower can be made more effective by using monitoring methods that can both detect and assess upset conditions. The multielectrode sensor may be used to predict corrosion based on the maximum anodic current from the sensor. As the directly measured maximum anodic current as shown in Figures 2 (Electrode #15) and 3 (Electrode #E6) depends on the information from only one of the many measured values and therefore has a greater uncertainty, statistical methods may be used to derive the maximum anodic current using the information from all the electrodes. In our previous analysis[18], the maximum anodic current, I_{max}, was estimated by:

$$I_{max} = k\sigma + I_{mean} \qquad (1)$$

Where σ is the standard deviation, k is a factor which depends on the sample size (or number of electrodes) and desired confidence interval and I_{mean} is the mean value of the currents from all the electrodes that are coupled together (I_{mean} should be equal to zero). Comparing the most anodic current in Figure 2 (Electrode #15) with the σ value in Figure 4 and the most anodic current in Figure 3

(Electrode #E6) with the σ value in Figure 5 at the time the sensor gave the highest corrosion signals, the ratios between the most anodic current and σ are 4.6 and 2.35 respectively. Similarly, the experimental data for Figures 7 and 8 show that the most anodic current to σ ratios are 4.0 and 2.5 respectively. As an estimate, this work uses 3 as the value for k in Eq 1 to determine the maximum anodic current of the sensor:

$$I_{max} = 3\sigma \qquad (2)$$

Knowing the maximum anodic current, the localized corrosion penetration rate may be estimated by[18]:

$$h_{max} = (f/\varepsilon)\, I_{max} W_E/(FA\rho) \qquad (3)$$

$$W_E = 1/\Sigma(m_i z_i/W_i) \qquad (4)$$

Where h_{max} is the estimated maximum penetration rate (cm/s), , f is the non-uniform factor which correct the effect of non-uniform attack on and the roughness of the surface of the most corroded miniature electrode, ε (ε<1) is the current distribution factor that represents the fraction of electrons from corrosion that flow to the other electrodes through the coupling circuit, W_E is the equivalent weight (g/mol), F is Faraday's constant (96485 C/eq), A is the surface area of the electrode (cm^2), ρ is the density of the alloy or electrode (g/cm^3), and m_i, z_i, and W_i are the mass fraction, oxidation state and atomic weight of component i in the electrode alloy, respectively. The values of both f and ε are dependent on the properties of the sensing electrodes and the corrosion environment. Work is in progress to determine the values of f and ε, and to examine the validity of Eq 3. The apparent maximum anodic current densities of the carbon steel sensing electrodes during the evaluation test for the Type A, Type B, Benzotriazole and sodium nitrate inhibitors are calculated, using Eq 2 and the apparent surface area ($0.1^2\pi/4=0.00785$ cm^2), and shown in Figure 9. As shown in Figure 9, the apparent maximum anodic current densities for the freshly polished (with 600-grit paper) carbon steel electrodes in aerated tap water are from $5x10^{-5}$ to $2x10^{-4}$ A/cm^2 in the first 20 hours of tests. The apparent maximum anodic current density decreased to $7x10^{-6}$, $1x10^{-6}$ A/cm^2 and $1x10^{-6}$ A/cm^2 after the addition of the Type A, Type B and Benzotriazole, respectively. Figure 9 also shows that there was no pronounced change in the apparent maximum anodic current density after the addition of $NaNO_3$. According to Figure 9, the order of effectiveness of the four corrosion inhibitors for carbon steel in cooling water is as follows:

Type B Inhibitor ≈ Benzotriazole > Type A Inhibitor >$NaNO_3$.

CONCLUSIONS

The performances of four types of corrosion inhibitors were evaluated for carbon steel in cooling water, using a coupled multielectrode localized corrosion sensor. The localized corrosion sensor provided a rapid real-time indication for the performance of the corrosion inhibitors. The measurement showed that the apparent maximum anodic current densities for the freshly polished carbon steel electrodes were from $5x10^{-5}$ to $2x10^{-4}$ A/cm^2 in aerated tap water during the first 20 hours of the tests. Upon the addition of either benzotriazole or a nitrite-based commercial corrosion inhibitor, the apparent maximum anodic current density was rapidly reduced to $1x10^{-6}$ A/cm^2.

Possible applications of the sensor include inhibitor selection and on-line monitoring. The differential response of the sensor to both inhibitor type and inhibitor concentration could provide useful

information in the selection of inhibitors. The rapid response of the sensor and the quantitative information provided in real-time would be useful for on-line monitoring of components that are not easily inspected. Because the sensor can be constructed using materials identical to the components that require monitoring, the sensor could be used in a wide range of applications

ACKNOWLEDGEMENTS

The experimental assistance by J. Aaron and technical discussions with O. Moghissi, S. Brossia and N. Sridhar are gratefully appreciated. The financial support for this work is provided by the Advisory Committee for Research of the Southwest Research Institute.

REFERENCES

1. H.S. Isaacs, U. Bertocci, J. Kruger, and S. Smialowska (Eds), Advances in Localized Corrosion (Houston, TX: NACE International, 1990).

2. L. Yang, X. Sun, and F. Steward, "An Electrical Resistance Probe for Monitoring Flow Assisted Corrosion in Simulated Primary Coolant of Nuclear Reactors at 310°C," Corrosion/99, Paper No. 459, (Houston, TX: NACE International,1999).

3. C.K. Brown, J.R. Davies, and B.J. Hemblade, "Real Time Metal Loss Internal Monitoring," Corrosion/2000, Paper No. 278, (Houston, TX: NACE International, 2000).

4. N. Sridhar, D.S. Dunn, C.S. Brossia, and O.C. Moghissi, "Corrosion Monitoring Techniques for Thermally Driven Wet and Dry Conditions," Corrosion/2000, Paper No. 283, (Houston, TX: NACE International, 2000).

5. F. Mansfeld, "The Polarization Resistance Technique for Measuring Corrosion Currents," in Advances in Corrosion Engineering and Technology, M. G. Fontana and R.W. Staehle (Eds), Vol. 6 (New York: Plenum, 1976), Chapter 3.

6. F. Mansfeld, "Polarization Resistance Measurements-Today's Status," in Electrochemical Techniques for Corrosion Engineering, R. Baboian Ed, (Houston, TX: NACE International, 1987).

7. A.N. Rothwell, D.A. Eden, and G. Row, "Electrochemical Noise Techniques for Determining Corrosion Rates and Mechanisms," Corrosion/92, Paper No. 223, (Houston, TX: NACE International, 1992).

8. J.A. Wharton, B. G. Mellor, R.J.K. Wood, and C.J. Smith, Journal of Electrochem. Society, 147, 9(2000), pp.3294-3301.

9. R.G. Kelly, M.E. Inman, and J.L. Hudson, "Analysis of Electrochemical Noise for Type 410 Stainless Steel in Chloride Solutions," in Electrochemical Noise Measurement for Corrosion Applications, J.R. Kearns, J.R. Scully, P.R. Roberge, D.L. Reichert, and J.L. Dawson (Eds.), Special Technical Publication 1277 (Conshohocken, PA: American Society for Testing and Materials, 1996), p. 101.

10. S.T. Pride, J. R. Scully, and J.L. Hudson, "Analysis of Electrochemical Noise from Metalstable Pitting in Aluminum, Aged Al-2%Cu, and AA 2024-T3," in Electrochemical Noise Measurement for Corrosion Applications, J.R. Kearns, J.R. Scully, P.R. Roberge, D.L. Reichert, and J.L. Dawson (Eds.), Special Technical Publication 1277 (Conshohocken, PA: American Society for Testing and Materials, 1996), p. 307.

11. B. Yang, "A Novel Method for On-line Determination of Underdeposit Corrosion Rate in Cooling Water Systems," Corrosion/94, Paper No. 335, (Houston, TX: NACE International, 1994).

12. B. Yang, "Localized Corrosion Monitoring in Cooling Water Systems," Corrosion/95, Paper No. 541, (Houston, TX: NACE International, 1995).

13. B. Yang, "Minimizing Localized Corrosion Via New Chemical Treatment and Performance Based Treatment Optimization and Control," Corrosion/99, Paper No. 307, (Houston, TX: NACE International, 1999).

14. B. Yang, "Real-time Localized Corrosion Monitoring in Refinery Cooling Water Systems," Corrosion/98, Paper No. 595, (Houston, TX: NACE International, 1998).

15. L. Yang, N. Sridhar, and O. Pensado, "Development of a Multielectrode Array Sensor for Monitoring Localized Corrosion," Presented at the 199th Meeting of the Electrochemical Society, Extended Abstract Volume I (Pennington, NJ: The Electrochemical Society, 2001), Abstract #182.

16. Y. J. Tan, "Wire Beam Electrode: A New Tool for Studying Localized Corrosion and Other Inheterogeinity Electrochemical Processes," Corrosion Science, 41, (1999), pp.226-247.

17. Y.J. Tan, S. Bailey, B. Kinsella, and A. Lowe, "Mapping Corrosion Kinetics Using the Wire Beam Electrode in Conjunction with Electrochemical Noise Resistance Measurements," J. of Electrochem. Soc., 147, 2(2000), pp. 530-539.

18. L. Yang, N. Sridhar, O. Pensado, and D. Dunn, "An In-situ Galvanically Coupled Multielectrode Array Sensor for Localized Corrosion," Submitted to Corrosion (2002).

19. Z. Szklarska-Smialowska, Pitting Corrosion of Metals (Houston, TX: NACE International, 1986).

20. J.E. Hoots, B.E. Morarty, B.F. Pesigan, and J.P. Rasimas, "Latest Methods of Performance Optimization and Control in Cooling Water," Corrosion/2001, Paper No. 01448, (Houston, TX: NACE International, 2001).

21. San Antonio Water System, Annual Water Quality Report (San Antonio, TX: San Antonio Water System, 2000).

Table 1 Typical Concentration Ranges of Substances in San Antonio Tap Water[21]

Substance	Concentration Range (ppm)
Calcium	74 – 102
Chloride	18 – 25
Magnesium	5 – 16
Sodium	10 – 15
Sulfate	21 – 29
Total Hardness (As Calcium Carbonate)	236 – 258
Total Alkalinity (As Calcium Carbonate)	202 – 252
Total Dissolved Solids	268 – 317
Nitrate	1.53 – 1.94
Fluoride	0.1 – 0.3

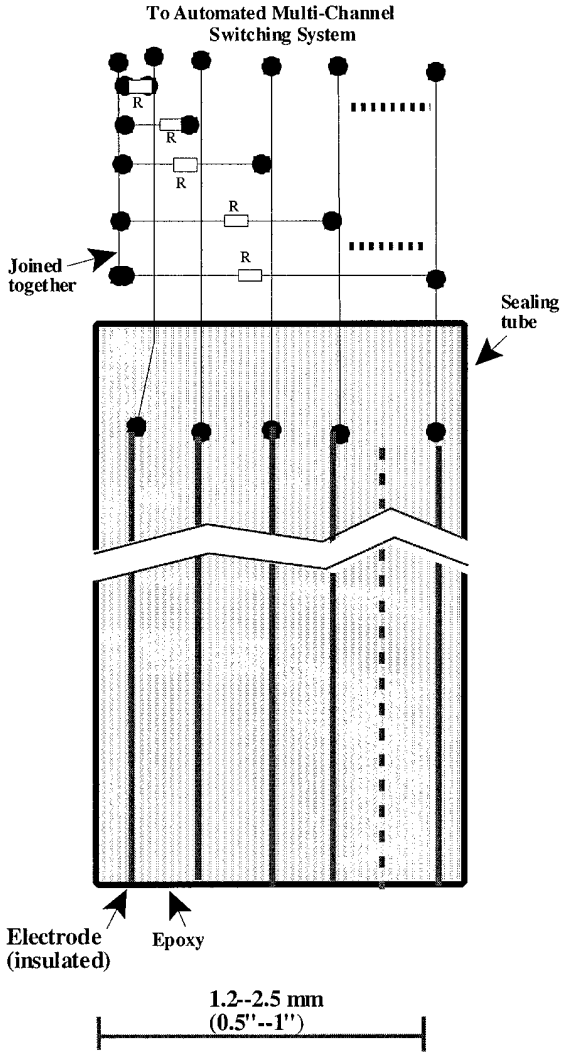

Figure 1 Schematic diagram of the coupled multielectrode array sensor for localized corrosion

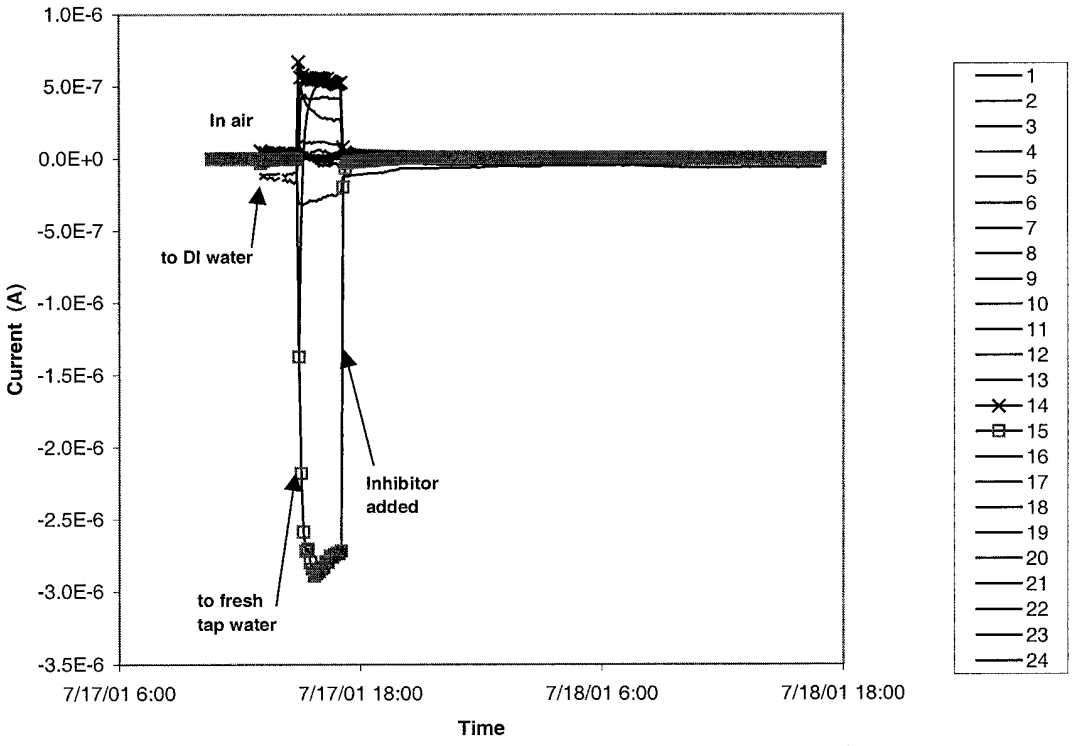

Figure 2 The response of the currents measured from a 24-electrode carbon steel sensor to the changes in chemical environments and the addition of the Type A commercial inhibitor.
Note: The legend shows the electrode numbers of the sensor

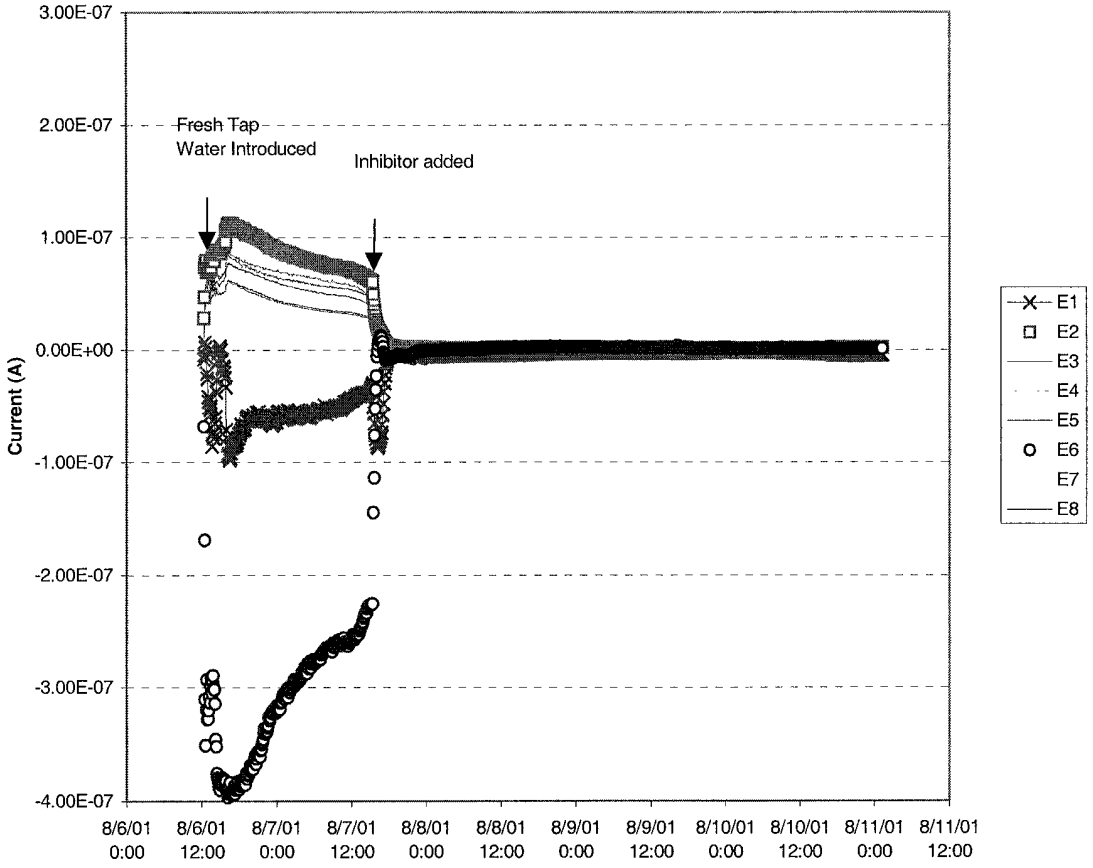

Figure 3 The response of the currents measured from an eight-electrode sensor to the addition of the Type B commercial inhibitor.

Note: The legend shows the electrode numbers of the sensor

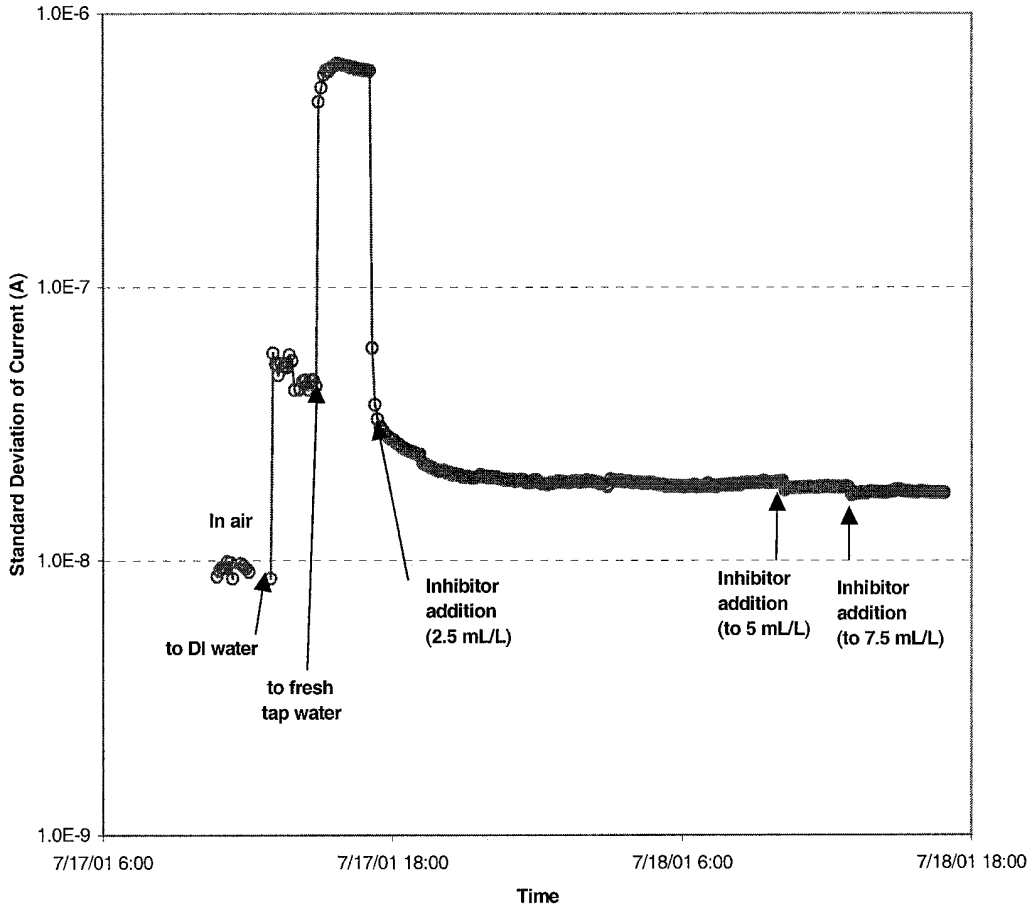

Figure 4 The response of the standard deviation of the 24 currents as shown in Figure 2 to the changes in chemical environments and the addition of the Type A commercial inhibitor

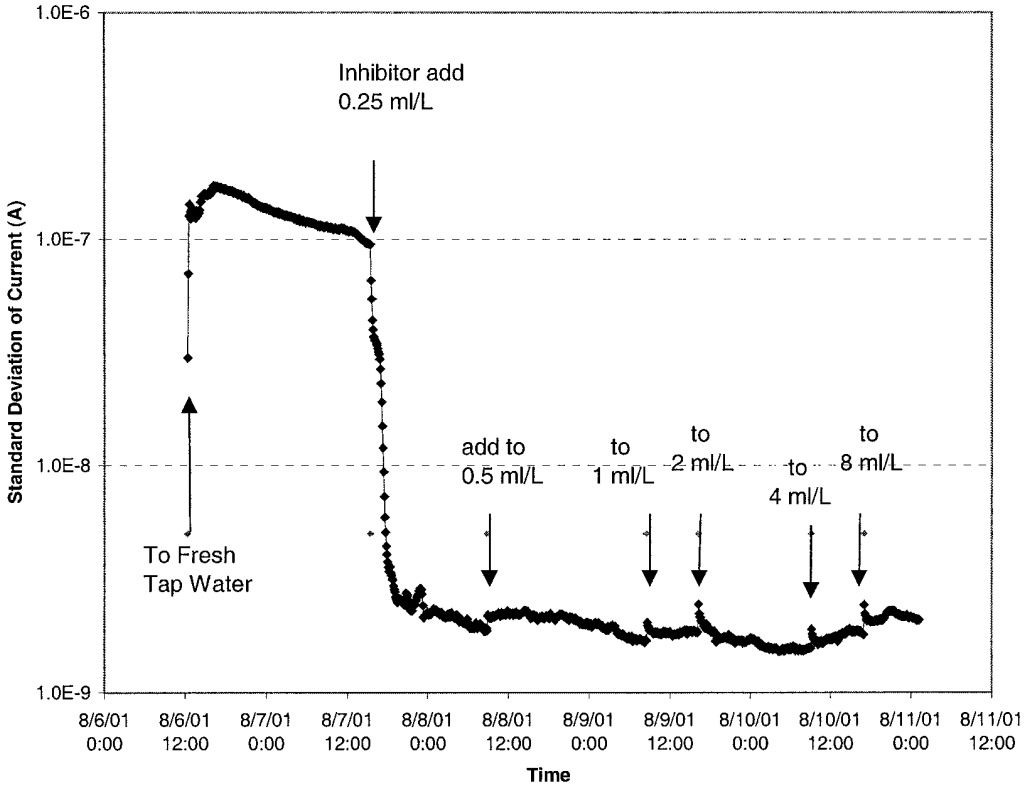

Figure 5 The response of the standard deviation of the eight currents as shown in Figure 3 to the addition of the Type B commercial inhibitor.

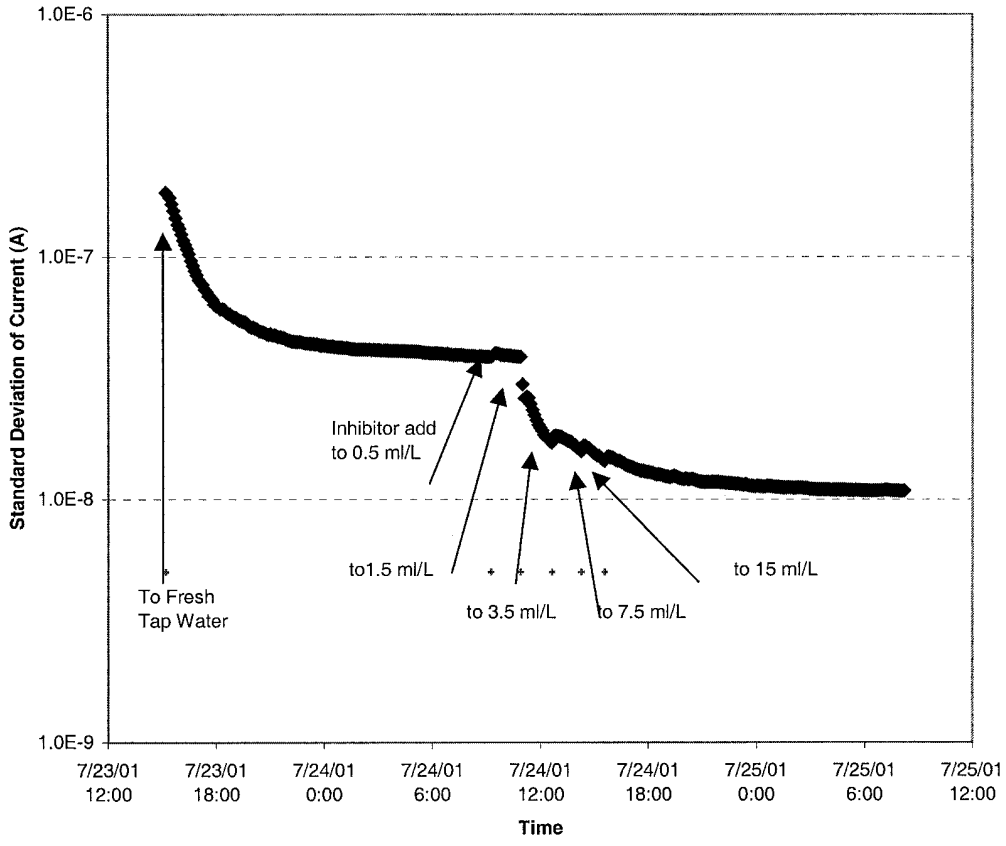

Figure 6 The response of the standard deviation of the 24-electrode sensor to the step changes of the concentration of Type A commercial inhibitor

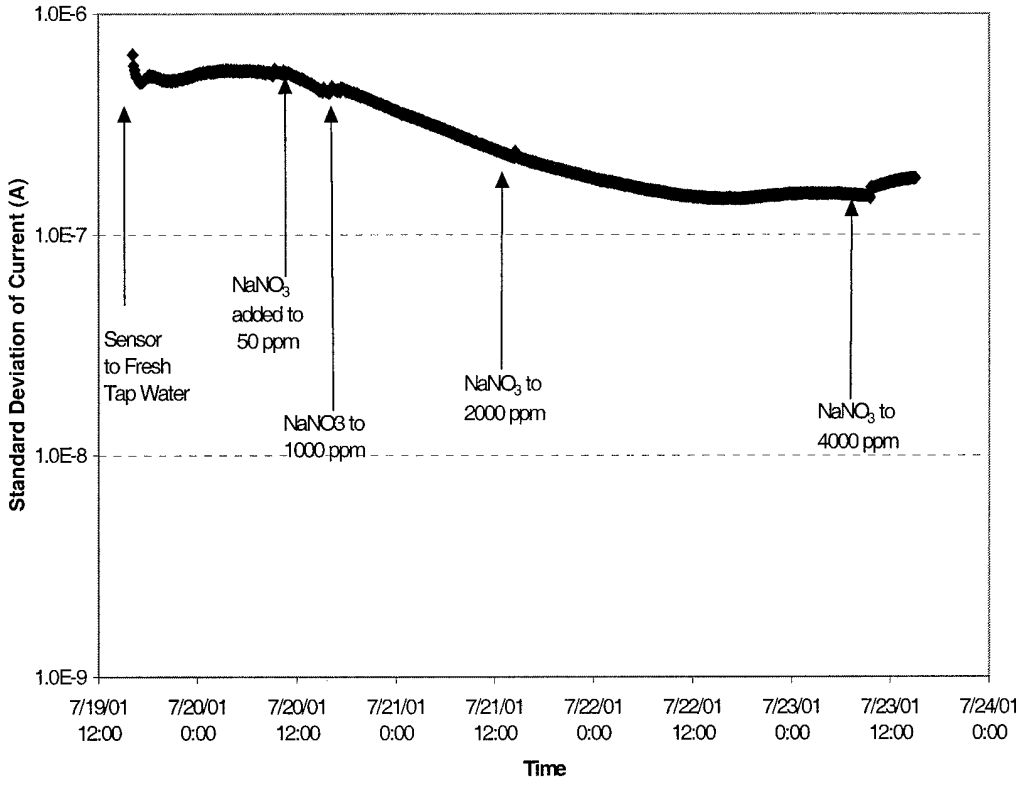

Figure 7 The response of the standard deviation of the currents measured from a 24-electrode sensor to the addition of the $NaNO_3$

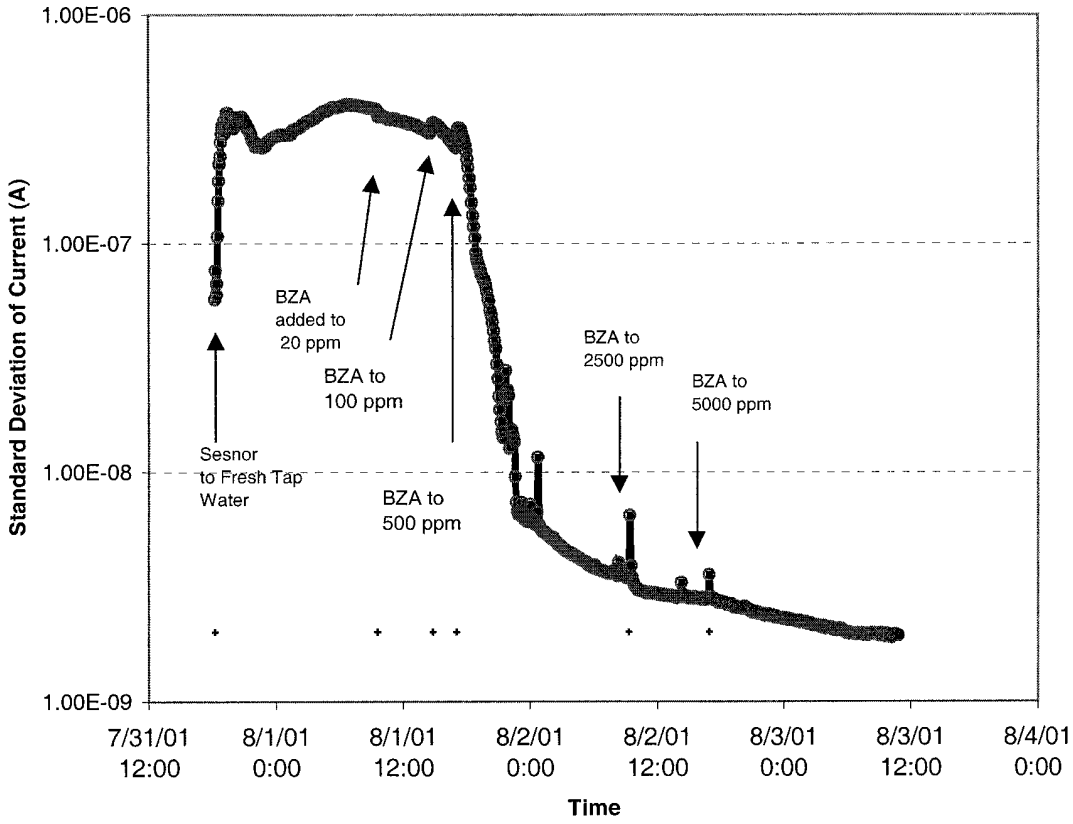

Figure 8 The response of the standard deviation of the currents measured from an eight-electrode sensor to the addition of the benzotriazole (BZA)

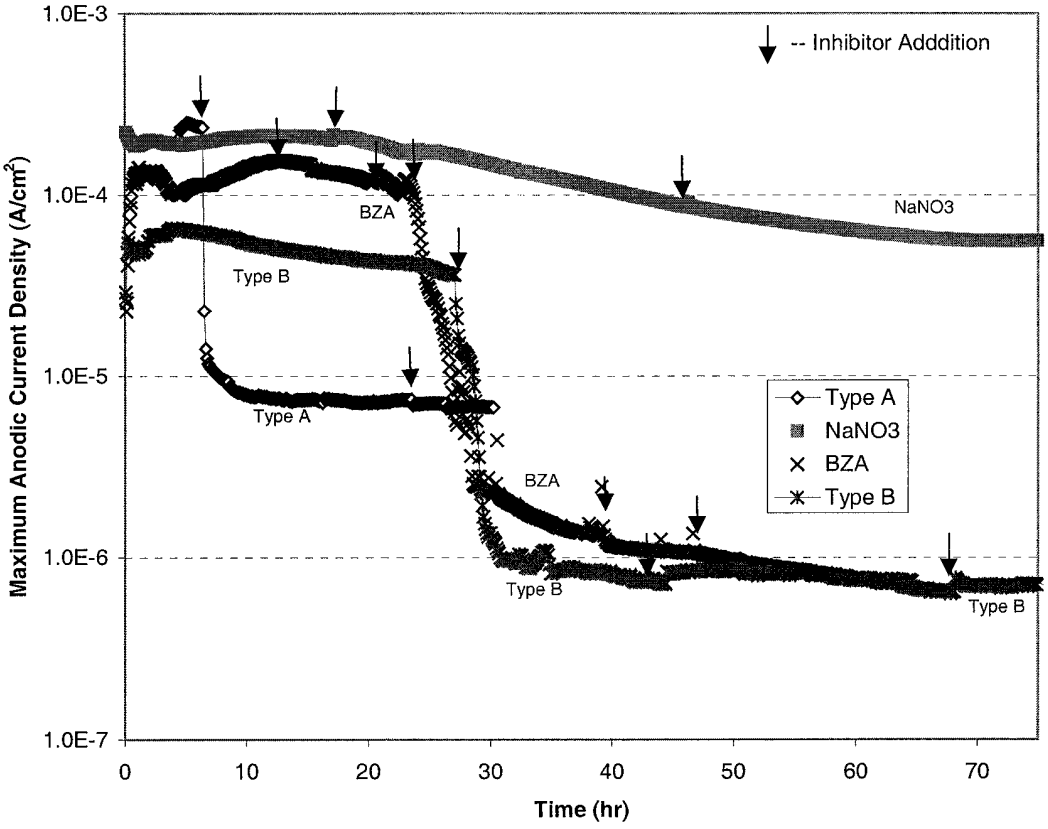

Figure 9 Responses of the apparent maximum anodic current densities of the 1010 carbon steel sensors to the addition of corrosion inhibitors in tap water.

Note: BZA - Benzotriazole